

Contributing to accurate high pressure viscosity measurements: vibrating wire viscometer and falling body viscometer techniques

Johnny R. Zambrano<sup>1,2</sup>, Manuel Sobrino<sup>1</sup>, M. Carmen Martín<sup>1</sup>, Miguel A. Villamañán<sup>1</sup>, César R. Chamorro<sup>1</sup>, José J. Segovia<sup>1\*</sup>

<sup>1</sup>TERMOCAL Research Group, Escuela de Ingenierías Industriales, Universidad de Valladolid, Paseo del Cauce 59, 47011 Valladolid, Spain

<sup>2</sup>Escuela Politécnica Nacional, Fac. de Ing. en Geología y Petróleos, Dpto. de Petróleos, Quito, Ecuador.

\*Corresponding author: e-mail: [jose.segovia@eii.uva.es](mailto:jose.segovia@eii.uva.es); fax number: +34 983 186462

KEYWORDS: Viscosity; Falling-body viscometer; Vibrating-wire viscometer; Toluene; n-Heptane; n-Dodecane.

#### ABSTRACT

Two new techniques for measuring viscosities at high pressure have been implemented at the TERMOCAL laboratory in order to obtain accurate values of thermophysical properties such as viscosity, especially at high pressures.

A vibrating-wire viscometer has been developed to accurately measure viscosities over the working ranges  $T = (283.15 \text{ to } 423.15) \text{ K}$  and  $p = (0.1 \text{ to } 140) \text{ MPa}$ . The setup of the equipment includes calibration with toluene and its validation with n-dodecane.

A falling body viscometer able to measure viscosities at  $T = (253.15 \text{ to } 523.15) \text{ K}$  and  $p = (0.1 \text{ to } 140) \text{ MPa}$  is also presented in this work. Results of calibration with toluene and its verification with n-heptane and n-dodecane are reported.

The detailed uncertainty budgets for both techniques are included in this work. Moreover, the paper studies the compatibility of the results obtained using both techniques according to their corresponding uncertainties in order to obtain reliable data. New viscosity measurements of 1,2,4-trimethylbenzene and 2,2,4-trimethylpentane have been performed and included in the paper.

## 1. Introduction

Most current techniques for measuring the viscosity of fluids require calibration with an appropriate reference fluid at the temperature and pressure measurement [1]. This imposes an upper limit on the achievable accuracy due to the lack of reference fluids, particularly at extreme pressures and temperatures. In fact, all viscosity measurements must be accredited in accordance with the viscosity of water at 20 °C under atmospheric pressure [2]. Yet, there is considerable controversy surrounding the value of the standard reference in these conditions, and there have been several new determinations of the property from the original measurement made in 1952 by Swindells et al. [3]. However, the viscosity value used as a reference has remained intact, despite its uncertainty [2].

Recent studies on viscosity revolve around two areas of great interest to researchers: developing techniques which can be used to determine viscosity over wide ranges of temperature, pressure and viscosity, and searching for standard liquids that can serve as a reference to calibrate

viscometers. Hence, our research group's interest in implementing two new viscometers which can work at high pressure based on different measurement principles.

## 2. Experimental section

### 2.1 Experimental techniques

#### 2.1.1 Vibrating wire viscometer (VWV)

The first technique is a vibrating wire viscometer. Its measurement principle consists of a circular section wire of radius  $R$ , length  $L$  ( $L \gg R$ ) and known density, tensioned and anchored at both ends [4]. It is surrounded by the fluid whose viscosity is being determined. The wire is oscillated on a plane perpendicular to its axis through an initial displacement in the initially stationary fluid. The equipment is used in forced mode, generating a disturbance and maintaining it in time. The resonance curve characteristics of the wire transverse oscillations are studied since they are determined by the viscosity and density of the fluid [5, 6].

The Navier-Stokes equation allows viscosity to be calculated using the frequency and the damping of the wire oscillatory motion, both in vacuum and in the fluid of interest. The mathematical model imposes certain conditions which can be taken into account when designing the equipment, and there is a correction since the wire is not immersed in an infinite sample volume [6, 7]. If the wire radius is measured accurately, no calibration liquid is necessary, such that it would be an absolute measuring method. The viscosity measurement range varies depending on the diameter of the wire used, such that the same equipment can operate in different ranges by simply changing the diameter, although it is still not possible to use it for

high viscosities. In recent years, studies have been conducted aimed at increasing the viscosity range of these techniques [8, 9]. Its main advantage is that it may be used to make absolute measurements or may be calibrated based on a small number of data.

The circulation of a constant sinusoidal current through the wire, combined with the constant magnetic field, produces the vibration of the wire. The electromotive force (EMF) generated through the vibrating wire can be measured with a lock-in amplifier in two stages, and is the sum of two complex terms  $V_1$  and  $V_2$  [10, 11].

$V_1$  is the voltage due to the electrical impedance of the fixed wire and is expressed by the following equation:

$$V_1 = a + ib + icf \quad (1)$$

where  $f$  is the frequency,  $i$  is the imaginary number and  $a$ ,  $b$ ,  $c$  are adjustable parameters determined by regression that account for the electrical impedance of the wire and absorb the offset used in the lock-in amplifier to ensure that the voltage signal is detected in the most sensitive range.

$V_2$  comes from the wire movement and is proportional to the speed of the wire. It is expressed by the following equation:

$$V_2 = \frac{i\Lambda f}{f_0 - (1 + \beta)f^2 + (\beta' + 2\Delta_0)f^2i} \quad (2)$$

where  $\Lambda$  is the amplitude,  $f$  is the driven frequency,  $f_0$  is the resonance frequency in vacuum,  $\Delta_0$  is the logarithmic decrement of the wire in vacuum,  $\beta = k \cdot \rho / \rho_s$  is the additional mass of the fluid

and  $\beta'$  the damping due to the fluid viscosity ( $\beta'=k'\cdot\rho/\rho_s$ );  $k$  and  $k'$  are functions of  $\Omega=(2\pi f\rho R^2)/\eta$ . Here,  $\rho$  and  $\eta$  are the density and the viscosity of the fluid, respectively, and  $R$  and  $\rho_s$  are the radius and density of the wire.

Using the approximation  $f_o^2 \approx (1 + \beta)f_r^2$ [12], viscosity can be expressed by equation (3):

$$\eta \approx \frac{\pi f_r R^2 \rho}{6} \left( \frac{f_b}{f_r} \right)^2 \left( 1 + \frac{\rho_s}{\rho} \right)^2 \quad (3)$$

$f_b$ , is the half-width of the resonance curve and  $f_r$  is the resonance frequency.

**Set-up and Calibration.** The vibrating-wire viscometer developed in the laboratory [13] allows dynamic viscosities up to 35 mPa·s to be measured in ranges  $T = (288.15 \text{ to } 423.15) \text{ K}$  and  $p = (0.1 \text{ to } 140) \text{ MPa}$ . A schematic view of the technique is shown in figure 1.

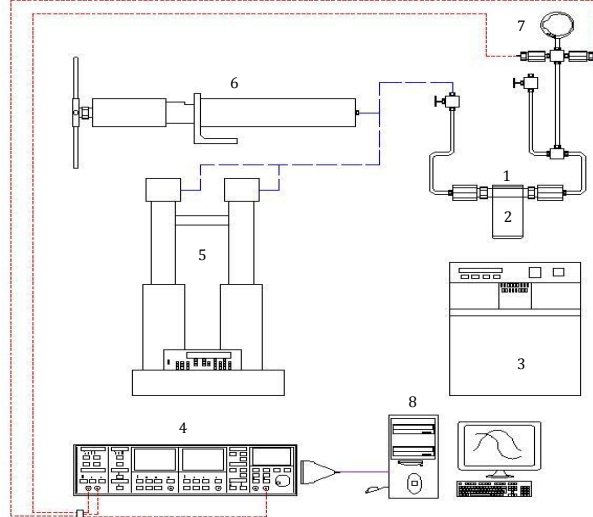


**Figure 1:** Schematic view of the technique: 1. Pressure vessel with the sensor inside 2. Magnet; 3. Thermostatic bath; 4. Lock-in amplifier; 5. Syringe pumps; 6. Pressurized cylinder 7. Digital manometer; 8. Computer.

The sensor is a tungsten wire (length 50 mm and nominal radius 75  $\mu\text{m}$ ) anchored at both ends (figure 2). It is inside a ceramic tube with a thermal expansion coefficient similar to the tungsten wire. Its dimensions are 48 mm length, 8 mm internal diameter and 10 mm external diameter, and it was designed and provided by Prof. J.P.M. Trusler of Imperial College London.

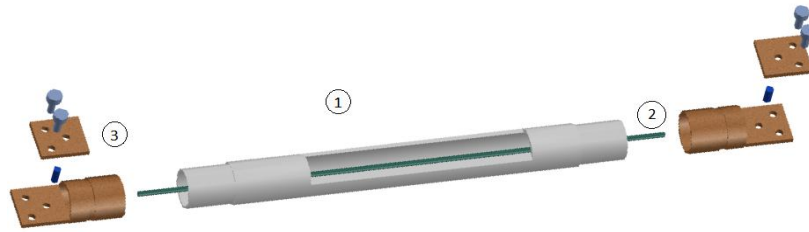


**Figure 2.** Vibrating-wire sensor: (1) flow tube; (2) tungsten wire; (3) support terminal, clamping plate, alignment pin, and M2 screws.

The sensor is placed inside a pressure vessel and both are mounted between the poles of the Al-Ni-Co-Fe magnet block with an “U” shape to maintain it in a constant external magnetic field.

The driven voltage and the wire response are measured by means of a Stanford Research Systems lock-in amplifier dual phase, digital signal processor (DSP), model SR830.

The temperature of the pressure vessel with the sensor is controlled with a thermostatic bath (Hart Scientific, model 6020) with an operating range from 20  $^{\circ}\text{C}$  to 300  $^{\circ}\text{C}$ . It is measured using a high precision ASL F100 thermometer and two Pt-100 calibrated and traceable to national standards with an extended uncertainty ( $k = 2$ ) of  $\pm 0.02$   $^{\circ}\text{C}$  at  $T = (-40 \text{ to } 230)^{\circ}\text{C}$ .

The system is pressurized using a variable volume control, HIP, model 68-5.75-10 and a GE Druck DPI104 digital manometer is used to measure pressure with an extended uncertainty ( $k = 2$ ) of  $\pm 0.02$  %. This was calibrated and traceable to national standards. The fluid can be loaded into the system manually or using ISCO syringe pumps 260D.

Measurements are performed using two different programs written in Agilent VEE-Pro V7.0. According to the calculation equation (3), the internal damping term,  $\Delta_0$ , and the radius of the wire,  $R_w$  should be calibrated first. Calibration of the internal damping term was performed in vacuum and ambient air. To obtain the radius of the wire,  $R_w$ , toluene was used since its properties are well-known.

**Uncertainty Budget.** Calculating the uncertainty of the vibrating-wire viscometer is based on the GUM 2008 document [14]. In order to apply the law of propagation of variances with explicit functions, equation (3) is used. This sets the dependence between the viscosity of the fluid inside the sensor and the oscillation frequency of the vibrating wire, as a function of variables:  $f_r$ ,  $R_w$ ,  $\rho$ ,  $f_b$ ,  $\rho_s$  (resonance frequency, wire radius, fluid density, bandwidth and wire density, respectively).

Thus, the standard uncertainty of the dynamic viscosity can be expressed as:

$$u(\eta(T, p)) = \left[ \left( \frac{\partial \eta(T, p)}{\partial f_r} \right)^2 u^2(f_r) + \left( \frac{\partial \eta(T, p)}{\partial R_w} \right)^2 u^2(R_w) + \left( \frac{\partial \eta(T, p)}{\partial \rho} \right)^2 u^2(\rho) + \left( \frac{\partial \eta(T, p)}{\partial f_b} \right)^2 u^2(f_b) + \left( \frac{\partial \eta(T, p)}{\partial \rho_s} \right)^2 u^2(\rho_s) \right]^{1/2} \quad (4)$$

Each variable depends on the experimental conditions  $T$ ,  $p$ , or both, as well as  $f_r(T, p)$ ,  $f_b(T, p)$ ,  $R_w(T)$ ,  $\rho_s(T)$ ,  $\rho(T, p)$ . Therefore, the contribution of partial uncertainties is evaluated for each variable under experimental conditions  $(T, p)$ .

Derivatives of equation (4) are specified in the following equations:

$$\frac{\partial \eta(T, p)}{\partial f_r} = -\frac{\pi R_w^2 f_b^2 (\rho + \rho_s)^2}{6 \rho f_r^2} = -\frac{\eta}{f_r} \quad (5)$$

$$\frac{\partial \eta(T, p)}{\partial R_w} = \frac{2\pi f_b^2 (\rho + \rho_s)^2 R_w R_w}{6 f_r \rho R_w} = \frac{2\eta}{R_w} \quad (6)$$

$$\frac{\partial \eta(T, p)}{\partial \rho} = \frac{\pi R_w^2 f_b^2}{6 f_r} \left(1 - \frac{\rho_s^2}{\rho^2}\right) = \frac{\eta(\rho - \rho_s)}{\rho(\rho + \rho_s)} \quad (7)$$

$$\frac{\partial \eta(T, p)}{\partial f_b} = \frac{2\pi R_w^2 (\rho + \rho_s)^2 f_b f_b}{6 f_r \rho f_b f_b} = \frac{2\eta}{f_b} \quad (8)$$

$$\frac{\partial \eta(T, p)}{\partial \rho_s} = \frac{2\pi R_w^2 f_b^2}{6 f_r} \left(1 + \frac{\rho_s}{\rho}\right) = \frac{2\eta}{(\rho + \rho_s)} \quad (9)$$

And the equation (4) is reformulated as equation (10):

$$u(\eta(T, p)) = \eta \left[ \left(-\frac{1}{f_r}\right)^2 u^2(f_r) + \left(\frac{2}{R_w}\right)^2 u^2(R_w) + \left(\frac{\rho - \rho_s}{\rho(\rho + \rho_s)}\right)^2 u^2(\rho) + \left(\frac{2}{f_b}\right)^2 u^2(f_b) + \left(\frac{2}{(\rho + \rho_s)}\right)^2 u^2(\rho_s) \right]^{1/2} \quad (10)$$

### 2.1.2 Falling body viscometer (FBV)

A falling body viscometer is apparatus whose working principle is based on measuring the time of a body falling through a vertical tube which contains the liquid being measured. The measuring cell was manufactured by Top Industrie following the design made by the “Groupe de Haute Pression, Laboratoire des Fluides Complexes” at the University of Pau in France [15].



However, the experimental setup and automation was developed in full at the TERMOCAL laboratory using high pressure equipment. It can measure viscosities in wide pressure and temperature ranges,  $p = (0.1 \text{ to } 140) \text{ MPa}$  and  $T = (253.15 \text{ to } 523.15) \text{ K}$ .

Assuming laminar flow and the body reaching its terminal velocity without eccentricity, equation (11), based on Stokes' law together with Newton's second law, could theoretically describe the behavior of this type of viscometers:

$$\eta = K \cdot \Delta\rho \cdot \Delta t \quad (11)$$

The terms of the equation are:  $\eta$  the viscosity,  $K$  a calibration constant which depends on the instrument and the falling body,  $\Delta\rho$  the difference between the density of the body material and the liquid density and finally,  $\Delta t$  the time recorded between the two coils.

Ideally,  $K$  could be determined without any calibration procedure using the instruments the known dimensions, the body mass and its density applying a mathematical expression. However, in practice, this is not advisable because the actual operation of the instrument departs from the simplified model given by said mathematical expression for many factors [16], which is why a calibration procedure is always performed in this sort of viscometer.

Several ways of calibration based on this model have been successfully applied: from the use of a single calibration constant modified by thermal expansion coefficients to the use of several calibration constants for each temperature and pressure set [17]. However, in our case, directly applying the model described by equation (11) has not allowed us to approach the study of viscosities because of its inability to reproduce the actual behavior of our viscometer in the range of viscosities herein studied (up to 1.3 mPa·s).

Given that viscosity ( $\eta$ ) depends on fall time ( $\Delta t$ ) and the difference between the falling body density and liquid density ( $\Delta\rho$ ), these terms must be present in our model. After several tests, the

best relationship found between viscosity ( $\eta$ ) and the characteristic variables ( $\Delta t$  and  $\Delta\rho$ ) could be the one expressed by:

$$\eta = a + b \cdot \Delta t \cdot \Delta\rho + c \cdot (\Delta t \cdot \Delta\rho)^2 \quad (12)$$

This equation, which has already been used for this kind of apparatus for low viscosity fluids, describes much more faithfully the behavior of our viscometer after applying correction at atmospheric pressure. The main difference from other authors is how we use it. As will be shown in the calibration procedure, we can apply the equation regardless of temperature and pressure. This is a major advantage since measurements can be performed with a single calibration curve under any temperature and any pressure conditions although measured viscosities must be within its viscosity calibration range.

**Set-up and calibration.** The core of falling body viscometers is the measuring cell. There are two concentric high pressure tubes of 400 mm in length. Both are filled with the pressurized fluid in order to maintain the same pressure inside and outside the inner tube, avoiding any possibility of deforming the tube. Four coils spaced 50 mm apart are arranged around the tube, and are placed towards the bottom of the tube in order to ensure that the terminal velocity of the body is reached when it passes through them. Both the tubes and the coils are surrounded by a thermostatic fluid from a thermostatic bath and the temperature of the system is measured by four Pt100 probes, calibrated and traceable to national standards with an extended uncertainty ( $k = 2$ ) of  $\pm 0.02$  °C at  $T = (-20 \text{ to } 120)$ °C.

Pressure is controlled using two different piston cylinders which can be operated manually or by means of a step by step motor. A digital Druck DPI 104 manometer is used to measure it with an extended uncertainty ( $k = 2$ ) of  $\pm 0.02$  %, calibrated and traceable to national standards.

The body used is a cylinder, with a hemispherical end, which is made of magnetic stainless steel to be detected by the coils. The density of the body, which can be considered approximately constant, was determined using a pycnometer, and its value was  $7.673 \text{ g}\cdot\text{cm}^{-3} \pm 0.017 \text{ g}\cdot\text{cm}^{-3}$ . The length of the body is 20 mm and its diameter is 6.35 mm. It goes through a tube which has an inner diameter of 6.52 mm. Therefore, the ratio between the inner diameter of the inner tube and the diameter of the falling body is 0.974, which is higher than the critical value of 0.93 established by Chen et al. [18] and also higher than the more conservative value of 0.95 established by Vant and cited by Schaschke et al. [19]. Working below these values might cause undesirable eccentricity effects.

As already mentioned, the coils are located towards the bottom of the tube to avoid any transient state and so as to favor terminal velocity being reached. In a previous work [20], it was proved that the time between the first and second coil is approximately the same as the time between the second and third coil, and the third and fourth coil for the most unfavorable case (lowest viscosities). This shows that terminal velocity is reached in all cases. For this reason, in order to avoid signal interferences between coils, the two intermediate coils are disconnected, and only the time between the first and the fourth coil, separated by 150 mm, is considered. The scheme of the cell is shown in figure 3.

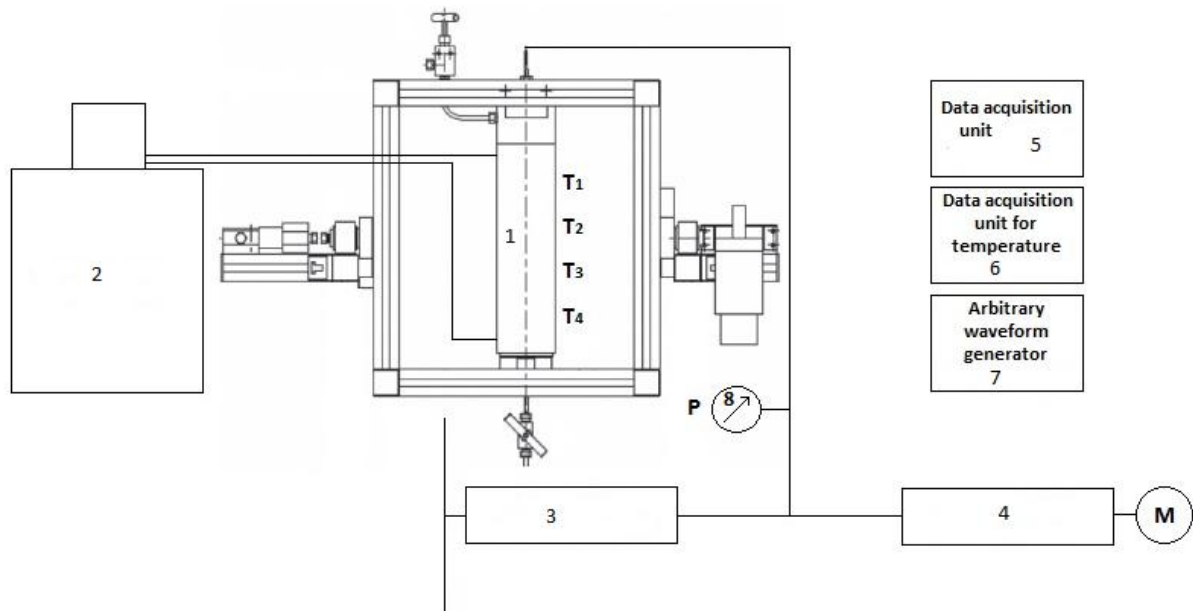


**Figure 3.** A schematic view of the falling body viscometer: 1. Measuring cell; 2. Thermostatic bath; Julabo F25-HE; 3. Manual high pressure generator; 4. Automatic high pressure generator; 5. Data acquisition unit Agilent U2352A; 6. Data acquisition unit for temperature Agilent 34970 A; 7. Arbitrary waveform generator Agilent 33220A; 8. Digital manometer.

Falling-time is determined using the signal detected by the coil detectors arranged along the tube, which has two circuits. The primary circuit is fed with a wave generator and the induced signal of the secondary circuit is detected by an oscilloscope.

The key to good performance in this type of viscometer is the accuracy of the measured times. In this sense, a time measurement system shown in Figure 4 was designed.

First, the arbitrary waveform generator Agilent 33220A provides a sinusoidal signal ( $2 V_{pp}$ , 450 Hz) which feeds primary coils, connected in parallel. Secondary coils are connected in phase opposition, such that the exit signal will be flat most of time except when the body passes through the coils. At that moment, the magnetic body generates a disturbance whose envelope

will provide us with the information required to obtain the falling time. This analog signal is digitized passing through the Multifunction Data Acquisition Unit (model Agilent U2352A), with an extended uncertainty ( $k = 2$ ) of  $\pm 0.01$  s. A fit is then made using polynomial functions and the last step consists of determining the relative extreme points of those functions so as to obtain the falling time.

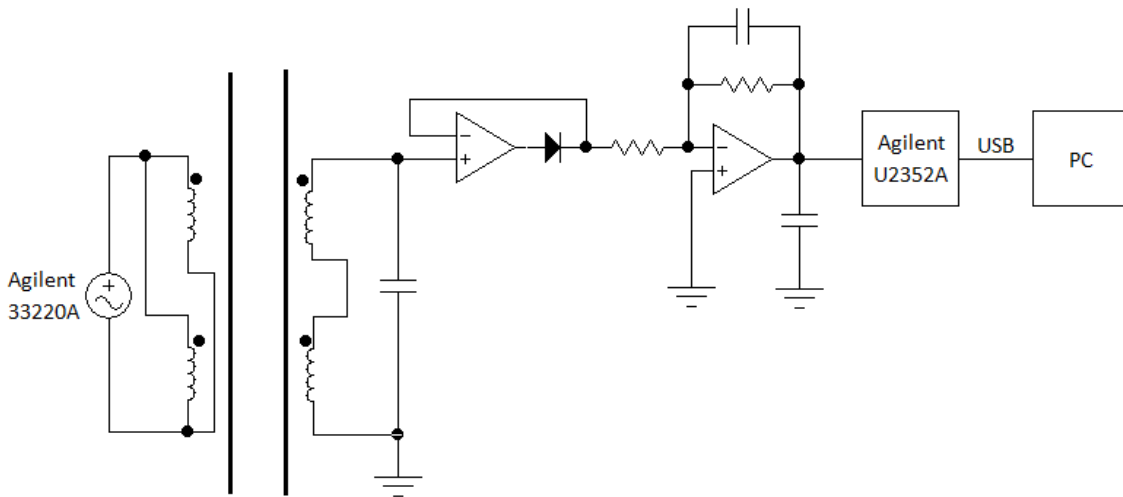


**Figure 4.** Time measurement system.

For this purpose, a computer program with chained loops using Agilent VEE Pro software was designed in full at the TERMOCAL laboratory to record all the parameters involved in our measurements. For an established temperature, different pressures are reached due to an automated pressure generator. For each pressure, time measurements are performed until a stability criterion has been achieved. The last five measurements of time must be within 1 %. This time measurement system is an important improvement for this kind of falling body technique, and provides accurate time measurements which will contribute to accurate viscosities.

Viscosity values will be obtained from the calibration curve by introducing the experimental falling time into the equation and, after that, adding a correction which is the difference between a reference viscosity and the viscosity from our model at atmospheric pressure for each isotherm. Reference viscosities at 0.1 MPa will be those measured using a vibrating wire viscometer. This is why we do not provide viscosity values at atmospheric pressure with this falling body equipment in the present work.

**Uncertainty Budget.** Calculating the uncertainty of the falling-body viscometer is based on the GUM 2008 document [14]. Equation (12) is used as a calibration model. The contribution associated to calibration function coefficients has two main parts, one associated to calibration parameters  $a$ ,  $b$ ,  $c$  (equations (13) to (16)) and the part associated to the independent variable of the fitting  $\Delta\rho\Delta t$  (equations (17) and (18)).

$$u_{a,b,c}(\eta) = \sqrt{u_a^2(\eta) + u_b^2(\eta) + u_c^2(\eta)} \quad (13)$$

$$u_a(\eta) = \frac{\partial\eta}{\partial a} \cdot u(a) = 1 \cdot u(a) \quad (14)$$

$$u_b(\eta) = \frac{\partial\eta}{\partial b} \cdot u(b) = (\Delta\rho\Delta t) \cdot u(b) \quad (15)$$

$$u_c(\eta) = \frac{\partial\eta}{\partial c} \cdot u(c) = (\Delta\rho\Delta t)^2 \cdot u(c) \quad (16)$$

$$u_{\Delta\rho\Delta t}(\eta) = \frac{\partial\eta}{\partial(\Delta\rho\Delta t)} \cdot u(\Delta\rho\Delta t) = (b + 2c\Delta\rho\Delta t) \cdot u(\Delta\rho\Delta t) \quad (17)$$

$$u(\Delta\rho\Delta t) = \frac{\partial(\Delta\rho\Delta t)}{\partial(\Delta\rho)} \cdot u(\Delta\rho) + \frac{\partial(\Delta\rho\Delta t)}{\partial(\Delta t)} \cdot u(\Delta t) = \Delta t \cdot u(\Delta\rho) + \Delta\rho \cdot u(\Delta t) \quad (18)$$

The uncertainty associated to calibration function coefficients will be the combination in terms of variances of the two parts described before, as shown in equation (19):

$$u_{calib}(\eta) = \sqrt{u_{a,b,c}^2(\eta) + u_{\Delta\rho\Delta t}^2(\eta)} \quad (19)$$

## 2.2 Materials

The following section provides the results obtained for the calibration of both techniques, the results of the uncertainty calculations and their validation through the viscosity measurements of some pure hydrocarbons. The characteristics of the pure compounds used in these measurements are summarized in table 1. The purity of the chemicals was checked by gas chromatography and all were used without further purification.

**Table 1.** Material description.

Chemical name	Source	Mass fraction purity <sup>a</sup>	Purification method
Dodecane	Sigma-Aldrich	≥0.99	None
Heptane	Sigma-Aldrich	≥0.995	None
Toluene	Sigma-Aldrich	≥0.998	None
1,2,4- Trimethylbenzene	Aldrich-Chemistry	≥0.997	None
2,2,4 Trimethylpentane	Sigma-Aldrich	≥0.995	None

<sup>a</sup> as stated by the supplier and checked by gas chromatography.

## 3. Results and discussion

### 3.1 Calibration and validation of the vibrating wire viscometer.

Although this technique can be used as an absolute method, better results are obtained when it is calibrated with the calculation of the wire radius,  $R_w$ , and the logarithmic decrement of the

wire in vacuum,  $\Delta_o$ , performing measurements in vacuum and in toluene at  $T = 293.15$  K and  $p = 0.1$  MPa. First,  $\Delta_o$  was determined in vacuum and then,  $R_w$  was obtained using toluene as reference fluid [21]. Results of the calibration and data used are summarized in table 2.

**Table 2.** Calibration data for the vibrating-wire viscometer through measurements in vacuum and toluene (calibration fluid) at  $T = 293.15$  K and  $p = 0.1$  MPa.

Nominal wire radius	$R$ ( $\mu\text{m}$ )	75
Length of wire	$L$ (mm)	50
Resonance frequency in vacuum	$f_o$ (Hz)	829.09
Logarithmic decrement of wire in vacuum	$\Delta_o \cdot 10^6$	214.5
Density of wire	$\rho_s$ ( $\text{kg}/\text{m}^3$ )	19300
Radius of wire, calibrated at 20 °C	$R_w$ ( $\mu\text{m}$ )	74.862
Resonance frequency in toluene	$f_r$ (Hz)	803.121
Bandwidth	$f_b$ (Hz)	18.513
Density of toluene [21]	$\rho$ ( $\text{kg}/\text{m}^3$ )	867.24
Dynamic viscosity of toluene [21]	$\eta$ (mPa·s)	0.5906

The uncertainty experimental viscosity obtained by the vibrating-wire viscometer has been estimated using equations (3), (4) and (10),. Due to the characteristics of the wire, the upper limit of the viscosity range is 35 mPa·s. The example shown in table 3 corresponds to the results for toluene at the highest pressure and lowest temperature working conditions. The estimated relative expanded uncertainty (k=2) is less than  $\pm 1.5\%$ .



**Table 3.** Uncertainty budget for the vibrating-wire viscometer for toluene at  $T = 293.15$  K and  $p = 140$  MPa

Amount ( $X_i$ )		$x_i$	Units	Probability Distribution	$u(x_i)$ : Standard Uncertainty	Sensitivity Coef. ( $c_i$ )	$u(y)$ : Uncertainty Contribution
Fluid	Viscosity	1.45	mPa·s	Normal			
Resonance	Calibration		Hz	Normal	0.012	0.0015	0.00002
frequency	Resolution	943	Hz	Rectangular	0.0003	0.0015	0.0000005
	Repeatability		Hz	Normal	0.01	0.0015	0.00002
Temperature	Calibration		K	Normal	0.01	0.022	0.0002
	Resolution	293.15	K	Rectangular	0.003	0.022	0.00006
	Uniformity		K	Rectangular	0.03	0.022	0.0006
	Stability		K	Rectangular	0.015	0.022	0.0003
Pressure	Calibration		MPa	Normal	0.014	0.12	0.0017
	Resolution	140	MPa	Rectangular	0.003	0.12	0.0004
	Stability		MPa	Rectangular	0.015	0.12	0.0018
Density	Solid	19300	kg·m <sup>-3</sup>	Normal	10	0.00014	0.0014
	Fluid	940	kg·m <sup>-3</sup>	Normal	0.3	0.00140	0.0005
Radius		75	mm	Normal	0.2	0.039	0.0078
Standard Uncertainty			mPa·s			$u(y)$	±0.0083
Relative Expanded Uncertainty ( $k=2$ )			100·(mPa·s/mPa·s)			$U_r(y)$	±1.5

It can be seen that the largest contributions to uncertainty are the densities of the fluid and the wire, the radius wire calibration and, due to the high pressure conditions, the pressure calibration.

The setup of the equipment includes the validation with toluene at eight isotherms  $T = (293.15$  to  $373.15)$  K and pressures up to 140 MPa and with n-dodecane at five isotherms  $T = (293.15$  to  $373.15)$  K and pressures up to 140 MPa. Experimental dynamic viscosities of toluene and n-dodecane are summarized in tables 4 and 5, respectively. The density values required for the calculations were obtained from the literature [22] or measured in the laboratory.

These experimental data were compared with the calculated values using the correlations published by Caudwell et al. [10] for n-dodecane and Assael et al. [21] for toluene. The standard deviation comparing the experimental data of the viscosity with literature values is 0.39 % for n-dodecane and 0.40 % for toluene. Both values are less than the expanded uncertainty ( $k = 2$ ) in the viscosity measurement which was estimated at less than 1.5 %. In figures 5 and 6 the relative deviations of the experimental data of n-dodecane and toluene with those calculated from literature are plotted and good agreement is observed.

**Table 4.** Experimental dynamic viscosity,  $\eta$  (mPa·s), for toluene at different temperatures  $T$ , and pressures  $p$  using the vibrating wire viscometer<sup>a</sup>

$T/\text{K}$	$p/\text{MPa}$	$\eta/\text{mPa}\cdot\text{s}$	$T/\text{K}$	$p/\text{MPa}$	$\eta/\text{mPa}\cdot\text{s}$	$T/\text{K}$	$p/\text{MPa}$	$\eta/\text{mPa}\cdot\text{s}$
293.15	0.1	0.5907	298.15	50.0	0.7983	323.15	0.1	0.4214
293.15	1.0	0.5928	298.15	60.0	0.8463	323.15	1.0	0.4238
293.15	5.0	0.6152	298.15	70.0	0.9027	323.15	5.0	0.4385
293.15	10.0	0.6387	298.15	80.0	0.9625	323.15	10.0	0.4551
293.15	20.0	0.6881	298.15	100.0	1.0811	323.15	20.0	0.4877
293.15	30.0	0.7354	298.15	120.0	1.2109	323.15	30.0	0.5293
293.15	40.0	0.7913	298.15	140.0	1.3488	323.15	40.0	0.5650
293.15	50.0	0.8532	313.15	0.1	0.4690	323.15	50.0	0.6021
293.15	60.0	0.9080	313.15	1.0	0.4746	323.15	60.0	0.6377
293.15	70.0	0.9632	313.15	5.0	0.4885	323.15	70.0	0.6789
293.15	80.0	1.0218	313.15	10.0	0.5046	323.15	80.0	0.7322
293.15	100.0	1.1493	313.15	20.0	0.5496	323.15	100.0	0.8090
293.15	120.0	1.2874	313.15	30.0	0.5914	323.15	120.0	0.9034
293.15	140.0	1.4558	313.15	40.0	0.6239	323.15	140.0	1.0041
298.15	0.1	0.5555	313.15	50.0	0.6704	333.15	0.1	0.3804
298.15	1.0	0.5603	313.15	60.0	0.7133	333.15	1.0	0.3856
298.15	5.0	0.5772	313.15	70.0	0.7572	333.15	5.0	0.3986
298.15	10.0	0.6006	313.15	80.0	0.8098	333.15	10.0	0.4153
298.15	20.0	0.6478	313.15	100.0	0.9082	333.15	20.0	0.4495
298.15	30.0	0.6920	313.15	120.0	1.0090	333.15	30.0	0.4794
298.15	40.0	0.7442	313.15	140.0	1.1281	333.15	40.0	0.5135

<sup>a</sup> Standard uncertainties  $u$  are  $u(T) = 0.01$  K,  $u_r(p) = 0.0001$  kPa/kPa and the combined relative expanded uncertainty  $U_{rc}$  is  $U_{rc}(\eta) = 0.015$  mPa·s/ mPa·s (0.95 level of confidence).

**Table 4.** (continued) Experimental dynamic viscosity,  $\eta$  (mPa·s), for toluene at different temperatures  $T$ , and pressures  $p$  using the vibrating wire viscometer<sup>a</sup>

$T/\text{K}$	$p/\text{MPa}$	$\eta/\text{mPa}\cdot\text{s}$	$T/\text{K}$	$p/\text{MPa}$	$\eta/\text{mPa}\cdot\text{s}$	$T/\text{K}$	$p/\text{MPa}$	$\eta/\text{mPa}\cdot\text{s}$
333.15	50.0	0.5485	353.15	0.1	0.3163	373.15	50.0	0.3876
333.15	60.0	0.5835	353.15	1.0	0.3177	373.15	60.0	0.4138
333.15	70.0	0.6187	353.15	5.0	0.3319	373.15	70.0	0.4372
333.15	80.0	0.6579	353.15	10.0	0.3449	373.15	80.0	0.4649
333.15	100.0	0.7353	353.15	20.0	0.3701	373.15	100.0	0.5193
333.15	120.0	0.8176	353.15	30.0	0.4006			
333.15	140.0	0.9111	353.15	40.0	0.4291			
348.15	0.1	0.3302	353.15	50.0	0.4620			
348.15	1.0	0.3361	353.15	60.0	0.4919			
348.15	5.0	0.3457	353.15	70.0	0.5176			
348.15	10.0	0.3588	353.15	80.0	0.5478			
348.15	20.0	0.3876	353.15	100.0	0.6113			
348.15	30.0	0.4180	353.15	120.0	0.6825			
348.15	40.0	0.4485	353.15	140.0	0.7550			
348.15	50.0	0.4795	373.15	0.1	0.2667			
348.15	60.0	0.5089	373.15	1.0	0.2671			
348.15	70.0	0.5441	373.15	5.0	0.2782			
348.15	80.0	0.5721	373.15	10.0	0.2893			
348.15	100.0	0.6407	373.15	20.0	0.3150			
348.15	120.0	0.7088	373.15	30.0	0.3401			
348.15	140.0	0.7836	373.15	40.0	0.3643			

<sup>a</sup> Standard uncertainties  $u$  are  $u(T) = 0.01$  K,  $u_r(p) = 0.0001$  kPa/kPa and the combined relative expanded uncertainty  $U_{rc}$  is  $U_{rc}(\eta) = 0.015$  mPa·s/ mPa·s (0.95 level of confidence).

**Table 5.** Experimental dynamic viscosity,  $\eta$  (mPa·s), for dodecane at different temperatures  $T$ , and pressures  $p$  using the vibrating wire viscometer<sup>a</sup>

$T/\text{K}$	$p/\text{MPa}$	$\eta/\text{mPa}\cdot\text{s}$	$T/\text{K}$	$p/\text{MPa}$	$\eta/\text{mPa}\cdot\text{s}$	$T/\text{K}$	$p/\text{MPa}$	$\eta/\text{mPa}\cdot\text{s}$
293.15	0.1	1.4907	313.15	0.1	1.0641	333.15	0.1	0.8013
293.15	1.0	1.5074	313.15	1.0	1.0744	333.15	1.0	0.8127
293.15	5.0	1.5864	313.15	5.0	1.1244	333.15	5.0	0.8550
293.15	10.0	1.6724	313.15	10.0	1.2006	333.15	10.0	0.8975
293.15	20.0	1.8769	313.15	20.0	1.3242	333.15	20.0	1.0008
293.15	30.0	2.0836	313.15	30.0	1.4755	333.15	30.0	1.0953
293.15	40.0	2.3101	313.15	40.0	1.6251	333.15	40.0	1.2161
293.15	50.0	2.5603	313.15	50.0	1.7785	333.15	50.0	1.3214
293.15	60.0	2.8216	313.15	60.0	1.9457	333.15	60.0	1.4401
293.15	70.0	3.1120	313.15	70.0	2.1286	333.15	70.0	1.5760
293.15	80.0	3.4276	313.15	80.0	2.3197	333.15	80.0	1.7068
293.15	100.0	4.1175	313.15	100.0	2.7576	333.15	100.0	1.9940
293.15	120.0	4.9531	313.15	120.0	3.2313	333.15	120.0	2.3016
293.15	140.0	5.8158	313.15	140.0	3.7547	333.15	140.0	2.6571

<sup>a</sup> Standard uncertainties  $u$  are  $u(T) = 0.01$  K,  $u_r(p) = 0.0001$  kPa/kPa and the combined relative expanded uncertainty  $U_{rc}$  is  $U_{rc}(\eta) = 0.015$  mPa·s/ mPa·s (0.95 level of confidence).

**Table 5.** (cont.) Experimental dynamic viscosity,  $\eta$  (mPa·s), for dodecane at different temperatures  $T$ , and pressures  $p$  using the vibrating wire viscometer<sup>a</sup>

$T/\text{K}$	$p/\text{MPa}$	$\eta/\text{mPa}\cdot\text{s}$	$T/\text{K}$	$p/\text{MPa}$	$\eta/\text{mPa}\cdot\text{s}$
353.15	0.1	0.6281	373.15	0.1	0.5055
353.15	1.0	0.6372	373.15	1.0	0.5149
353.15	5.0	0.6713	373.15	5.0	0.5392
353.15	10.0	0.7053	373.15	10.0	0.5743
353.15	20.0	0.7819	373.15	20.0	0.6286
353.15	30.0	0.8694	373.15	30.0	0.7003
353.15	40.0	0.9528	373.15	40.0	0.7715
353.15	50.0	1.0366	373.15	50.0	0.8425
353.15	60.0	1.1230	373.15	60.0	0.9100
353.15	70.0	1.2126	373.15	70.0	0.9844
353.15	80.0	1.3124	373.15	80.0	1.0656
353.15	100.0	1.5316	373.15	100.0	1.2199
353.15	120.0	1.7568	373.15	120.0	1.4019
353.15	140.0	2.0233	373.15	140.0	1.5880

<sup>a</sup> Standard uncertainties  $u$  are  $u(T) = 0.01$  K,  $u_r(p) = 0.0001$  kPa/kPa and the combined relative expanded uncertainty  $U_{rc}$  is  $U_{rc}(\eta) = 0.015$  mPa·s/ mPa·s (0.95 level of confidence).

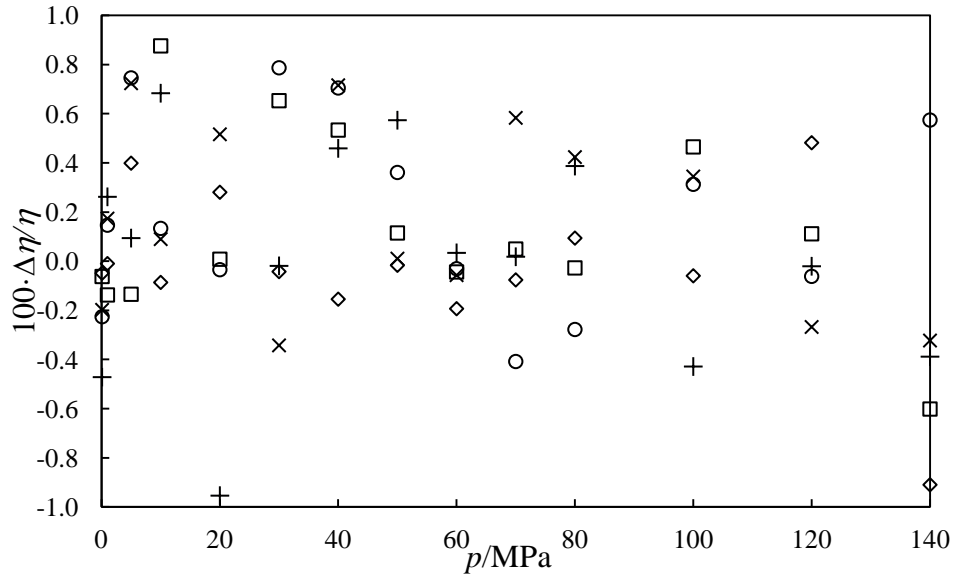


**Figure 5.** Relative differences  $\Delta\eta/\eta = \{\eta(\text{exp}) - \eta(\text{lit})\} / \eta(\text{lit})$  of the experimental viscosity of n-dodecane compared to the literature values of Caudwell et al. [10] as a function of pressure at different temperatures ( $\diamond$  293.15 K;  $\square$  313.15 K;  $\times$  333.15 K;  $\circ$  353.15 K;  $+$  373.15 K).

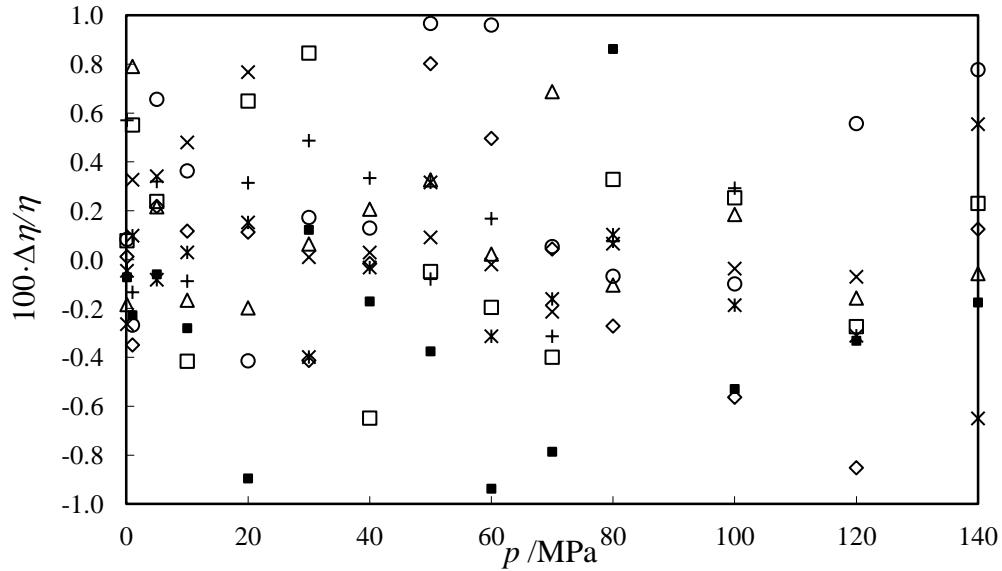


**Figure 6.** Relative differences  $\Delta\eta/\eta = \{\eta(\text{exp}) - \eta(\text{lit})\} / \eta(\text{lit})$  of the experimental viscosity of toluene compared to the literature values of Assael et al. [21] as a function of pressure at different temperatures ( $\diamond$  293.15 K;  $*$  298.15 K;  $\square$  313.15 K;  $\blacksquare$  323.15 K;  $\times$  333.15 K;  $\Delta$  348.15 K;  $\circ$  353.15 K;  $+$  373.15 K)

### 3.2 Calibration and validation of the falling body viscometer.

Calibration of the falling body viscometer was performed from  $p = (0.1 \text{ to } 120) \text{ MPa}$  at  $T = (293.15, 313.15, 333.15, 353.15) \text{ K}$  using toluene as calibration fluid [21].

Fall time was recorded (five repetitions for each pressure and temperature) and its behavior as a function of pressure could be fitted to a second degree polynomial for each isotherm. The second step of calibration then involves fitting all those points (figure 7) using the model expressed by equation (12).



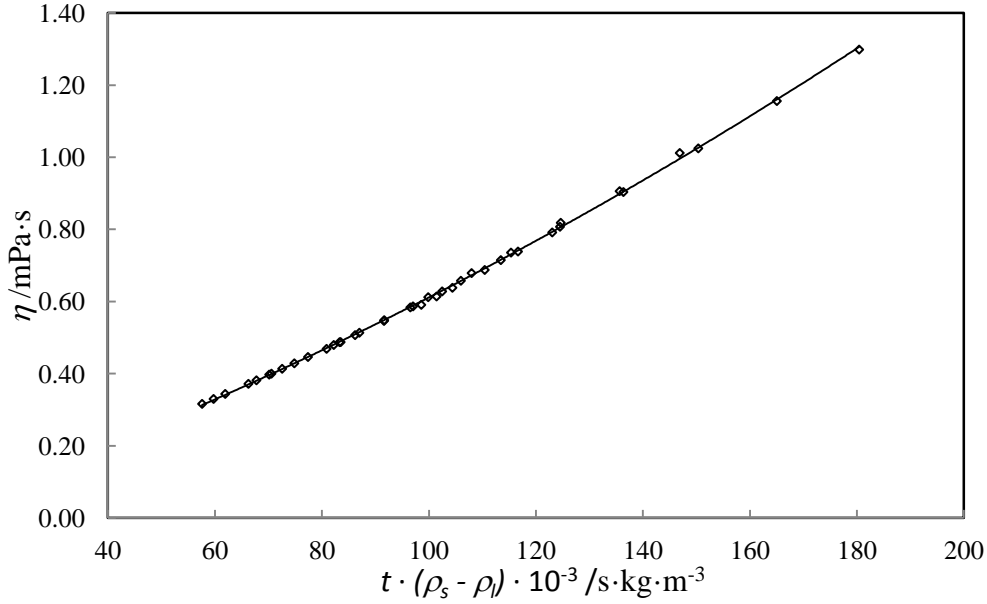


**Figure 7.** Calibration curve, equation (12) for the falling body viscometer using toluene [21] as reference fluid.

The values of the parameters of equation (12) and their standard deviations are summarized in table 6. Standard deviation of the fitting was  $5.0 \cdot 10^{-3}$  mPa·s.

**Table 6.** Coefficients  $a$ ,  $b$ ,  $c$  of the fitting equation (12) and standard error ( $\sigma$ ).

	value	$\sigma$
$a/ \text{mPa} \cdot \text{s}$	$-1.756 \cdot 10^{-2}$	$9.1 \cdot 10^{-3}$
$b/ \text{mPa} \cdot \text{m}^3 \cdot \text{kg}^{-1}$	$4.985 \cdot 10^{-6}$	$1.7 \cdot 10^{-7}$
$c/ \text{mPa} \cdot \text{m}^6 \cdot \text{kg}^{-2} \cdot \text{s}^{-1}$	$1.3025 \cdot 10^{-11}$	$7.5 \cdot 10^{-13}$

Worth noting is that the smallest viscosity value considered in this calibration is 0.31 mPa·s (toluene at 353.15 K and 0.1 MPa conditions) and the highest viscosity value is 1.30 mPa·s (toluene at 293.15 K and 120 MPa conditions), such that all values of viscosity which we calculate using this calibration must lie between those values.

Uncertainty calculation based on the model expressed by equation (12) is shown in tables 7 and 8 for two measurements in the limits of the viscosity range. Considering a normal distribution with a coverage factor  $k = 2$  (confidence level of 95.45 %), the relative expanded uncertainty varies from  $\pm 4.0$  % for the most viscous point to  $\pm 4.9$  % for the least viscous point. These values concur with the values given by other authors [23].

**Table 7.** Uncertainty budget for the falling body viscometer for 2,2,4-trimethylpentane at  $T = 293.15$  K and  $p = 100$  MPa

Amount (Xi)	$x_i$	Units	Probability Distribution	$u(x_i)$ : Standard Uncertainty	Sensitivity Coef. ( $c_i$ )	$u(\eta)$ : Uncertainty Contribution	
Reference	Viscosity	1.30	mPa·s	Normal	0.013	1	0.013
Time	Calibration	26	s	Normal	0.005	0.064	0.00032
	Resolution		s	Rectangular	0.0029	0.064	0.00019
	Repeatability		s	Normal	0.12	0.064	0.0074
Temperature	Calibration	293.15	K	Normal	0.010	0.014	0.00014
	Resolution		K	Rectangular	0.0029	0.014	0.000039
	Uniformity		K	Rectangular	0.029	0.014	0.00039
	Stability		K	Rectangular	0.014	0.014	0.00020
Pressure	Calibration	100	MPa	Normal	0.01	0.0091	0.000091
	Resolution		MPa	Rectangular	0.0029	0.0091	0.000026
	Stability		MPa	Rectangular	0.014	0.0091	0.00013
Density	Solid	7673	kg·m <sup>-3</sup>	Normal	17	0.00026	0.0045
	Fluid	757.94	kg·m <sup>-3</sup>	Normal	1.9	0.00014	0.00027
Calibration function coefficients			mPa·s	Normal	0.021	1	0.021
Standard Uncertainty			mPa·s			$u(\eta)$	0.026
Relative Expanded Uncertainty ( $k=2$ )			100·(mPa·s/mPa·s)			$U_r(\eta)$	4.0 %

**Table 8.** Uncertainty budget for the falling body viscometer for 2,2,4-trimethylpentane at  $T = 333.15$  K and  $p = 5$  MPa

Amount ( $X_i$ )	$x_i$	Units	Probability Distribution	$u(x_i)$ : Standard Uncertainty	Sensitivity Coef. ( $c_i$ )	$u(\eta)$ : Uncertainty Contribution	
Reference	Viscosity	0.35	mPa·s	Normal	0.0035	1	0.0035
Time	Calibration	9	s	Normal	0.010	0.046	0.0005
	Resolution		s	Rectangular	0.0029	0.046	0.00013
	Repeatability		s	Normal	0.040	0.046	0.0018
Temperature	Calibration	333.15	K	Normal	0.010	0.0042	0.000042
	Resolution		K	Rectangular	0.0029	0.0042	0.000012
	Uniformity		K	Rectangular	0.029	0.0042	0.00012
	Stability		K	Rectangular	0.014	0.0042	0.000060
Pressure	Calibration	5	MPa	Normal	0.0005	0.0046	0.0000023
	Resolution		MPa	Rectangular	0.0029	0.0046	0.000013
	Stability		MPa	Rectangular	0.014	0.0046	0.000067
Density	Solid	7673	kg·m <sup>-3</sup>	Normal	17	0.000061	0.0010
	Fluid	664.69	kg·m <sup>-3</sup>	Normal	1.7	0.000046	0.000077
Calibration function coefficients			mPa·s	Normal	0.0075	1	0.0075
Standard Uncertainty			mPa·s			$u(\eta)$	0.0085
Relative Expanded Uncertainty ( $k=2$ )			100·(mPa·s/mPa·s)			$U_r(\eta)$	4.9 %

n-Heptane and n-dodecane are the substances chosen to test the calibration presented above. Experimental data of dynamic viscosities of n-heptane at  $T = (293.15, 313.15)$  K and n-dodecane at  $T = (313.15, 333.15, 353.15)$  K are shown in table 9.

**Table 9.** Experimental dynamic viscosity,  $\eta$  (mPa·s), for n-heptane and n-dodecane at different temperatures  $T$ , and pressures  $p$  using the falling body viscometer<sup>a</sup>

n-Heptane			n-Heptane			n-Dodecane		
$T/K$	$p/MPa$	$\eta/mPa\cdot s$	$T/K$	$p/MPa$	$\eta/mPa\cdot s$	$T/K$	$p/MPa$	$\eta/mPa\cdot s$
293.15	5.0	0.4359	313.15	5.0	0.3564	313.15	5.0	1.1345
293.15	10.0	0.4603	313.15	10.0	0.3756	313.15	10.0	1.2184
293.15	20.0	0.5074	313.15	20.0	0.4131	333.15	5.0	0.8518
293.15	30.0	0.5517	313.15	30.0	0.4518	333.15	10.0	0.9030
293.15	40.0	0.5949	313.15	40.0	0.4899	333.15	20.0	1.0019
293.15	60.0	0.6912	313.15	60.0	0.5683	333.15	30.0	1.1118
293.15	80.0	0.7864	313.15	80.0	0.6498	333.15	40.0	1.2227
293.15	100.0	0.9027	313.15	100.0	0.7309	353.15	5.0	0.6657
293.15	120.0	1.0307	313.15	120.0	0.8186	353.15	10.0	0.7047
						353.15	20.0	0.7791
						353.15	30.0	0.8651
						353.15	40.0	0.9597
						353.15	60.0	1.1212

<sup>a</sup> Standard uncertainties  $u$  are  $u(T) = 0.01$  K,  $u_r(p) = 0.0001$  kPa/kPa and the combined relative expanded uncertainty  $U_{rc}$  is  $U_{rc}(\eta) = 0.049$  mPa·s/ mPa·s (0.95 level of confidence).

With regard to *n*-heptane, the correlation proposed by Assael et al. [22] was used to compare our experimental viscosities in order to check the technique. For *n*-dodecane viscosities, the correlation proposed by Caudwell et al. [10] was used. Densities for both

compounds were taken from the literature [24]. Relative deviations from the literature are plotted in figure 8, and show that these deviations are always smaller than the uncertainty of the apparatus.

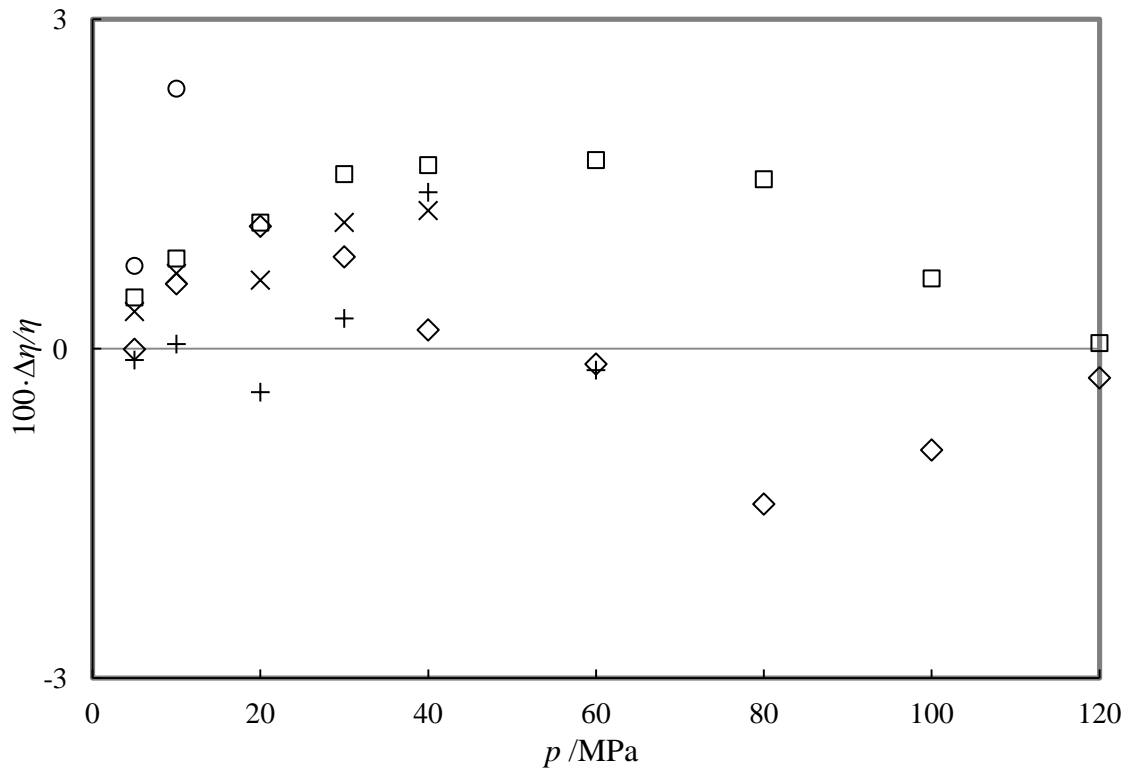


**Figure 8.** Relative differences  $\Delta\eta/\eta = \{\eta(\text{exp}) - \eta(\text{lit})\} / \eta(\text{lit})$  of the experimental viscosity of n-heptane and n-dodecane compared to literature values at different temperatures: ◇ n-heptane at  $T = 293.15$  K in comparison with Assael et al. [22]; □ n-heptane at  $T = 313.15$  K in comparison with Assael et al. [22]; ○ n-dodecane at  $T = 313.15$  K in comparison with Caudwell et al. [10]; × n-dodecane at  $T = 333.15$  K in comparison with Caudwell et al. [10]; + n-dodecane at  $T = 353.15$  K in comparison with Caudwell et al. [10].

### 3.3 Other Hydrocarbon Measurements

In this section, viscosity measurements performed for 2,2,4-trimethylpentane and 1,2,4-trimethylbenzene using both techniques are presented and compared.

Before presenting these data, table 10 contains the dynamic viscosities of n-heptane determined using the vibrating wire viscometer. The root mean square deviation between these values and those calculated using the correlation given by Assael et al. [22] is 0.24 %, which is lower than the estimated uncertainty of the measurements.

In addition, these data were compared with other values of the literature obtaining different absolute average deviations: 1.5% in comparison with Pensado et al. [25], 1.8% in comparison with Zeberg-Mikkelsen et al. [26], or 1.1% in comparison with Sagdeev et al. [27], most of the deviations are in coherence with the uncertainties declared by the authors.

**Table 10.** Experimental dynamic viscosity,  $\eta$  (mPa·s), for n-heptane at different temperatures  $T$ , and pressures  $p$  using the vibrating wire viscometer<sup>a</sup>

$T/\text{K}$	$p/\text{MPa}$	$\eta/\text{mPa}\cdot\text{s}$	$T/\text{K}$	$p/\text{MPa}$	$\eta/\text{mPa}\cdot\text{s}$	$T/\text{K}$	$p/\text{MPa}$	$\eta/\text{mPa}\cdot\text{s}$
293.15	0.1	0.4151	298.15	0.1	0.3914	313.15	0.1	0.3379
293.15	1.0	0.4202	298.15	1.0	0.3962	313.15	1.0	0.3412
293.15	5.0	0.4354	298.15	5.0	0.4142	313.15	5.0	0.3540
293.15	10.0	0.4579	298.15	10.0	0.4329	313.15	10.0	0.3735
293.15	20.0	0.5013	298.15	20.0	0.4756	313.15	20.0	0.4074
293.15	30.0	0.5459	298.15	30.0	0.5175	313.15	30.0	0.4462
293.15	40.0	0.5950	298.15	40.0	0.5613	313.15	40.0	0.4806
293.15	50.0	0.6406	298.15	50.0	0.6081	313.15	50.0	0.5208
293.15	60.0	0.6927	298.15	60.0	0.6535	313.15	60.0	0.5563
293.15	70.0	0.7446	298.15	70.0	0.7026	313.15	70.0	0.5992
293.15	80.0	0.7965	298.15	80.0	0.7519	313.15	80.0	0.6400
293.15	100.0	0.9106	298.15	100.0	0.8572	313.15	100.0	0.7259
293.15	120.0	1.0284	298.15	120.0	0.9720	313.15	120.0	0.8176
293.15	140.0	1.1602	298.15	140.0	1.0889	313.15	140.0	0.9137

<sup>a</sup> Standard uncertainties  $u$  are  $u(T) = 0.01$  K,  $u_r(p) = 0.0001$  kPa/kPa and the combined relative expanded uncertainty  $U_{rc}$  is  $U_{rc}(\eta) = 0.015$  mPa·s/ mPa·s (0.95 level of confidence).



**Table 10.** (Cont) Experimental dynamic viscosity,  $\eta$  (mPa·s), for n-heptane at different temperatures  $T$ , and pressures  $p$  using the vibrating wire viscometer<sup>a</sup>

$T/\text{K}$	$p/\text{MPa}$	$\eta/\text{mPa}\cdot\text{s}$	$T/\text{K}$	$p/\text{MPa}$	$\eta/\text{mPa}\cdot\text{s}$	$T/\text{K}$	$p/\text{MPa}$	$\eta/\text{mPa}\cdot\text{s}$
333.15	0.1	0.2821	353.15	0.1	0.2406	363.15	0.1	0.2224
333.15	1.0	0.2844	353.15	1.0	0.2435	363.15	1.0	0.2254
333.15	5.0	0.2965	353.15	5.0	0.2549	363.15	5.0	0.2374
333.15	10.0	0.3121	353.15	10.0	0.2672	363.15	10.0	0.2493
333.15	20.0	0.3415	353.15	20.0	0.2957	363.15	20.0	0.2757
333.15	30.0	0.3746	353.15	30.0	0.3216	363.15	30.0	0.2996
333.15	40.0	0.4061	353.15	40.0	0.3493	363.15	40.0	0.3252
333.15	50.0	0.4355	353.15	50.0	0.3730	363.15	50.0	0.3504
333.15	60.0	0.4681	353.15	60.0	0.4019	363.15	60.0	0.3754
333.15	70.0	0.5022	353.15	70.0	0.4304	363.15	70.0	0.3978
333.15	80.0	0.5337	353.15	80.0	0.4570	363.15	80.0	0.4243
333.15	100.0	0.6030	353.15	100.0	0.5119	363.15	100.0	0.4782
333.15	120.0	0.6736	353.15	120.0	0.5735	363.15	120.0	0.5314
333.15	140.0	0.7509	353.15	140.0	0.6335	363.15	140.0	0.5865

<sup>a</sup> Standard uncertainties  $u$  are  $u(T) = 0.01$  K,  $u_r(p) = 0.0001$  kPa/kPa and the combined relative expanded uncertainty  $U_{rc}$  is  $U_{rc}(\eta) = 0.015$  mPa·s/ mPa·s (0.95 level of confidence).

Finally, the experimental dynamic viscosities for 2,2,4-trimethylpentane using the vibrating wire viscometer or the falling body viscometer are summarized in tables 11 and 12, respectively. In addition, tables 13 and 14 contain the dynamic viscosities for 1,2,4-trimethylbenzene for both techniques.

**Table 11.** Experimental dynamic viscosity,  $\eta$  (mPa·s), for 2,2,4-trimethylpentane at different temperatures  $T$ , and pressures  $p$  using the vibrating wire viscometer<sup>a</sup>

$T/\text{K}$	$p/\text{MPa}$	$\eta/\text{mPa}\cdot\text{s}$	$T/\text{K}$	$p/\text{MPa}$	$\eta/\text{mPa}\cdot\text{s}$	$T/\text{K}$	$p/\text{MPa}$	$\eta/\text{mPa}\cdot\text{s}$
293.15	0.1	0.5064	298.15	50.0	0.8154	323.15	0.1	0.3645
293.15	1.0	0.5100	298.15	60.0	0.8956	323.15	1.0	0.3694
293.15	5.0	0.5399	298.15	70.0	0.9815	323.15	5.0	0.3915
293.15	10.0	0.5733	298.15	80.0	1.0698	323.15	10.0	0.4157
293.15	20.0	0.6366	298.15	100.0	1.2345	323.15	20.0	0.4640
293.15	30.0	0.7059	298.15	120.0	1.4345	323.15	30.0	0.5146
293.15	40.0	0.7817	298.15	140.0	1.6480	323.15	40.0	0.5714
293.15	50.0	0.8608	313.15	0.1	0.4035	323.15	50.0	0.6255
293.15	60.0	0.9567	313.15	1.0	0.4114	323.15	60.0	0.6832
293.15	70.0	1.0416	313.15	5.0	0.4353	323.15	70.0	0.7420
293.15	80.0	1.1268	313.15	10.0	0.4633	323.15	80.0	0.7969
293.15	100.0	1.3157	313.15	20.0	0.5177	323.15	100.0	0.9249
293.15	120.0	1.5180	313.15	30.0	0.5775	323.15	120.0	1.0679
293.15	140.0	1.7391	313.15	40.0	0.6351	323.15	140.0	1.2102
298.15	0.1	0.4746	313.15	50.0	0.6902	333.15	0.1	0.3265
298.15	1.0	0.4819	313.15	60.0	0.7509	333.15	1.0	0.3296
298.15	5.0	0.5090	313.15	70.0	0.8173	333.15	5.0	0.3515
298.15	10.0	0.5388	313.15	80.0	0.8861	333.15	10.0	0.3754
298.15	20.0	0.6027	313.15	100.0	1.0450	333.15	20.0	0.4216
298.15	30.0	0.6672	313.15	120.0	1.1953	333.15	30.0	0.4705
298.15	40.0	0.7394	313.15	140.0	1.3627	333.15	40.0	0.5232

<sup>a</sup> Standard uncertainties  $u$  are  $u(T) = 0.01$  K,  $u_r(p) = 0.0001$  kPa/kPa and the combined relative expanded uncertainty  $U_{rc}$  is  $U_{rc}(\eta) = 0.015$  mPa·s/ mPa·s (0.95 level of confidence).

**Table 11.** (continued) Experimental dynamic viscosity,  $\eta$  (mPa·s), for 2,2,4-trimethylpentane at different temperatures  $T$ , and pressures  $p$  using the vibrating wire viscometer<sup>a</sup>

$T/\text{K}$	$p/\text{MPa}$	$\eta/\text{mPa}\cdot\text{s}$	$T/\text{K}$	$p/\text{MPa}$	$\eta/\text{mPa}\cdot\text{s}$	$T/\text{K}$	$p/\text{MPa}$	$\eta/\text{mPa}\cdot\text{s}$
333.15	50.0	0.5790	348.15	0.1	0.2829	353.15	0.1	0.2738
333.15	60.0	0.6246	348.15	1.0	0.2863	353.15	1.0	0.2748
333.15	70.0	0.6779	348.15	5.0	0.3060	353.15	5.0	0.2923
333.15	80.0	0.7280	348.15	10.0	0.3274	353.15	10.0	0.3175
333.15	100.0	0.8361	348.15	20.0	0.3692	353.15	20.0	0.3570
333.15	120.0	0.9606	348.15	30.0	0.4131	353.15	30.0	0.3966
333.15	140.0	1.0951	348.15	40.0	0.4565	353.15	40.0	0.4379
			348.15	50.0	0.5022	353.15	50.0	0.4853
			348.15	60.0	0.5476	353.15	60.0	0.5294
			348.15	70.0	0.6049	353.15	70.0	0.5738
			348.15	80.0	0.6507	353.15	80.0	0.6288
			348.15	100.0	0.7538	353.15	100.0	0.7176
			348.15	120.0	0.8640	353.15	120.0	0.8245
			348.15	140.0	0.9770	353.15	140.0	0.9332

<sup>a</sup> Standard uncertainties  $u$  are  $u(T) = 0.01$  K,  $u_r(p) = 0.0001$  kPa/kPa and the combined relative expanded uncertainty  $U_{rc}$  is  $U_{rc}(\eta) = 0.015$  mPa·s/ mPa·s (0.95 level of confidence).

**Table 12.** Experimental dynamic viscosity,  $\eta$  (mPa·s), for 2,2,4-trimethylpentane at different temperatures  $T$ , and pressures  $p$  using the falling body viscometer<sup>a</sup>

$T/\text{K}$	$p/\text{MPa}$	$\eta/\text{mPa}\cdot\text{s}$	$T/\text{K}$	$p/\text{MPa}$	$\eta/\text{mPa}\cdot\text{s}$	$T/\text{K}$	$p/\text{MPa}$	$\eta/\text{mPa}\cdot\text{s}$
293.15	5	0.5412	313.15	5	0.4251	333.15	5	0.3468
293.15	10	0.5744	313.15	10	0.4517	333.15	10	0.3700
293.15	20	0.6401	313.15	20	0.5129	333.15	20	0.4153
293.15	30	0.7047	313.15	30	0.5662	333.15	30	0.4590
293.15	40	0.7738	313.15	40	0.6128	333.15	40	0.5083
293.15	60	0.9262	313.15	60	0.7307	333.15	60	0.6083
293.15	80	1.1148	313.15	80	0.8553	333.15	80	0.6981
293.15	100	1.2975	313.15	100	1.0242	333.15	100	0.8101
			313.15	120	1.1845	333.15	120	0.9406

<sup>a</sup> Standard uncertainties  $u$  are  $u(T) = 0.01$  K,  $u_r(p) = 0.0001$  kPa/kPa and the combined relative expanded uncertainty  $U_{rc}$  is  $U_{rc}(\eta) = 0.049$  mPa·s/ mPa·s (0.95 level of confidence).

In the case of the 2,2,4-trimethylpentane, there are literature data available for comparison [28-30]. The relative deviations between experimental and literature data are shown graphically in Figure 9. This comparison is done with the values obtained with the vibrating wire viscometer since they are measured at the same temperatures.

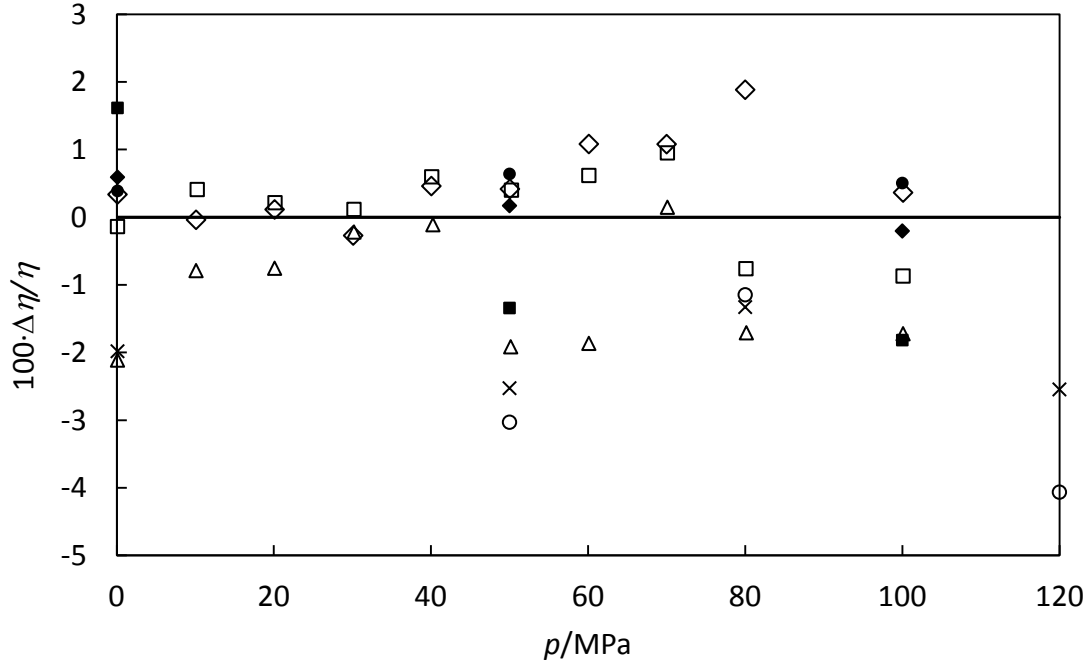


Figure 9: Relative differences  $\Delta\eta/\eta = \{\eta(\text{exp}) - \eta(\text{lit})\} / \eta(\text{lit})$  of the experimental viscosity of 2,2,4-trimethylpentane compared to literature values at different temperatures: ◆ at  $T = 298$  K, ■ at  $T = 323$  K and ● at  $T = 348$  K in comparison with Dymond et al. [28]; × at  $T = 298$  K and ○ at  $T = 353$  K in comparison with Krahn et al. [29]; ◇ at  $T = 298$  K, □ at  $T = 323$  K and △ at  $T = 348$  K in comparison with Padua et al. [30].

It can be observed the good agreement of our data with those of the literature, the average absolute deviations were: 0.8 % in comparison with Dymond et al. [28], 1 % in comparison with Krahn et al. [29] and 0.5 % in comparison with Padua et al. [30] which were also measured using a vibrating wire viscometer.

**Table 13.** Experimental dynamic viscosity,  $\eta$  (mPa·s), for 1,2,4-trimethylbenzene at different temperatures  $T$ , and pressures  $p$  using the vibrating wire viscometer<sup>a</sup>

$T/\text{K}$	$p/\text{MPa}$	$\eta/\text{mPa}\cdot\text{s}$	$T/\text{K}$	$p/\text{MPa}$	$\eta/\text{mPa}\cdot\text{s}$	$T/\text{K}$	$p/\text{MPa}$	$\eta/\text{mPa}\cdot\text{s}$
293.15	0.1	0.8929	313.15	50.0	1.0264	353.15	0.1	0.4527
293.15	1.0	0.9065	313.15	60.0	1.0996	353.15	1.0	0.4566
293.15	5.0	0.9417	313.15	70.0	1.1708	353.15	5.0	0.4711
293.15	10.0	0.9769	313.15	80.0	1.2493	353.15	10.0	0.4886
293.15	20.0	1.0610	313.15	100.0	1.4146	353.15	20.0	0.5283
293.15	30.0	1.1479	313.15	120.0	1.5986	353.15	30.0	0.5626
293.15	40.0	1.2332	313.15	140.0	1.8238	353.15	40.0	0.5993
293.15	50.0	1.3362	333.15	0.1	0.5596	353.15	50.0	0.6375
293.15	60.0	1.4349	333.15	1.0	0.5646	353.15	60.0	0.6768
293.15	70.0	1.5664	333.15	5.0	0.5885	353.15	70.0	0.7177
293.15	80.0	1.6926	333.15	10.0	0.6066	353.15	80.0	0.7606
293.15	100.0	1.9518	333.15	20.0	0.6476	353.15	100.0	0.8518
293.15	120.0	2.2875	333.15	30.0	0.6942	353.15	120.0	0.9515
293.15	140.0	2.6681	333.15	40.0	0.7426	353.15	140.0	1.0646
313.15	0.1	0.6989	333.15	50.0	0.7922			
313.15	1.0	0.7096	333.15	60.0	0.8456			
313.15	5.0	0.7359	333.15	70.0	0.9004			
313.15	10.0	0.7606	333.15	80.0	0.9675			
313.15	20.0	0.8203	333.15	100.0	1.0938			
313.15	30.0	0.8894	333.15	120.0	1.2212			
313.15	40.0	0.9528	333.15	140.0	1.3427			

<sup>a</sup> Standard uncertainties  $u$  are  $u(T) = 0.01$  K,  $u_r(p) = 0.0001$  kPa/kPa and the combined relative expanded uncertainty  $U_{rc}$  is  $U_{rc}(\eta) = 0.015$  mPa·s/ mPa·s (0.95 level of confidence).

**Table 14.** Experimental dynamic viscosity,  $\eta$  (mPa·s), for 1,2,4-trimethylbenzene at different temperatures  $T$ , and pressures  $p$  using the falling body viscometer<sup>a</sup>

$T/\text{K}$	$p/\text{MPa}$	$\eta/\text{mPa}\cdot\text{s}$	$T/\text{K}$	$p/\text{MPa}$	$\eta/\text{mPa}\cdot\text{s}$	$T/\text{K}$	$p/\text{MPa}$	$\eta/\text{mPa}\cdot\text{s}$
293.15	5	0.9130	333.15	5	0.5819	353.15	5	0.4715
293.15	10	0.9568	333.15	10	0.6058	353.15	10	0.4920
293.15	20	1.0420	333.15	20	0.6529	353.15	20	0.5320
293.15	30	1.1370	333.15	30	0.7014	353.15	30	0.5710
293.15	40	1.2242	333.15	40	0.7504	353.15	40	0.6125
313.15	5	0.7254	333.15	60	0.8467	353.15	60	0.6967
313.15	10	0.7531	333.15	80	0.9594	353.15	80	0.7819
313.15	20	0.8131	333.15	100	1.0858	353.15	100	0.8778
313.15	30	0.8704	333.15	120	1.2282	353.15	120	0.9727
313.15	40	0.9344						
313.15	60	1.0697						
313.15	80	1.2496						

<sup>a</sup> Standard uncertainties  $u$  are  $u(T) = 0.01$  K,  $u_r(p) = 0.0001$  kPa/kPa and the combined relative expanded uncertainty  $U_{rc}$  is  $U_{rc}(\eta) = 0.049$  mPa·s/ mPa·s (0.95 level of confidence).

An interesting analysis is to establish a comparison between FBV and VWV experimental results. In this sense, viscosities of n-heptane, n-dodecane, 2,2,4-trimethylpentane and 1,2,4-trimethylbenzene shown before for the FBV will be compared with their corresponding values of the VWV.

The comparison of these 87 values is presented in figure 10. Uncertainties of FBV are considered to vary linearly between the values discussed before. It can be seen that all the deviations are within the lines which represent FBV uncertainties (the maximum is 4.1 % for 2,2,4-trimethylpentane at 333.15 K and 80 MPa). This implies full agreement of the results obtained by both techniques.

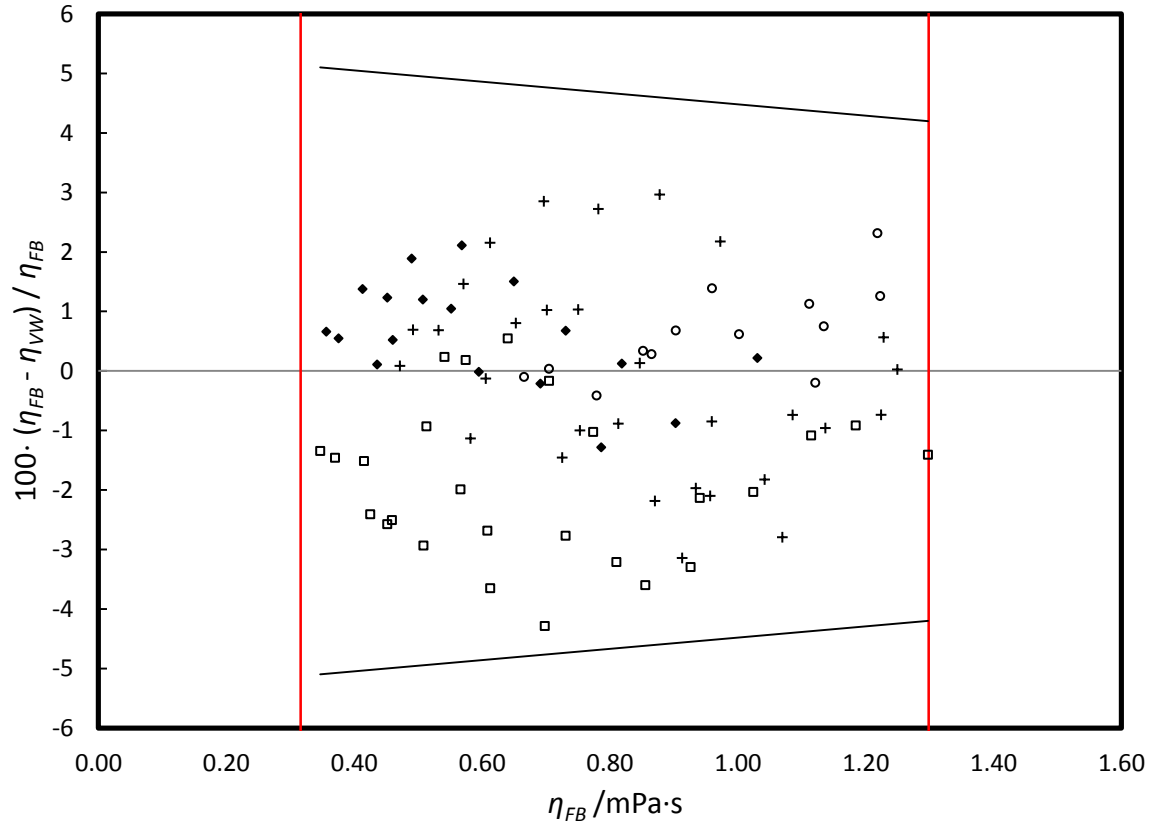


**Figure 10.** Relative deviations on viscosity measurements using a falling body viscometer (FB) or a vibrating wire viscometer (VW) as a function of the viscosity determined by means of the falling body viscometer for different hydrocarbons:  $\blacklozenge$  n-heptane;  $\circ$  n-dodecane;  $\square$  2,2,4-trimethylpentane;  $+$  1,2,4-trimethylbenzene. The vertical red lines represent the limit of the viscosity measurements and the grey lines represent the uncertainty of the falling body viscometer.



#### 4. Conclusions

A vibrating-wire viscometer (VWV) has been developed (assembled and calibrated) at the TERMOCAL research group laboratory, for accurate measurement of dynamic viscosities of fluids in the range  $T = (283.15 \text{ to } 423.15) \text{ K}$  and  $p = (0.1 \text{ to } 140) \text{ MPa}$ .

Measurements in vacuum, with air and with toluene at 293.15 K at 0.1 MPa were performed in order to calibrate the radius of the wire ( $R_w = 75.0793 \text{ }\mu\text{m}$ ) and to determine its natural logarithmic decrease in vacuum ( $\Delta_o = 44.8 \cdot 10^{-6}$ ).

Rigorous uncertainty calculations were carried out to measure dynamic viscosity, said estimations giving an expanded relative uncertainty ( $k = 2$ ) of less than  $\pm 1.5 \%$ . The standard deviations obtained when our measurements are compared with the literature are always less than the uncertainty of the measurements.

A falling-body viscometer (FBV) which is able to measure dynamic viscosities of liquids from  $p = (0.1 \text{ to } 140) \text{ MPa}$  and  $T = (253.15 \text{ to } 523.15) \text{ K}$  has been developed in parallel with the vibrating wire viscometer.

Calibration of the falling body equipment was performed with toluene in a temperature range  $T = (293.15 \text{ to } 353.15)$  and pressures up to 120 MPa, allowing us to measure fluids in a low viscosity range between 0.31 mPa·s and 1.30 mPa·s.

A detailed study of uncertainties was performed and relative expanded uncertainties ( $k = 2$ ) between  $\pm 4.0 \%$  (1.30 mPa·s) and  $\pm 4.9 \%$  (0.31 mPa·s) were obtained.

The falling body viscometer was validated using n-heptane and n-dodecane and most deviations were within  $\pm 2 \%$  compared to the literature, far from uncertainty limits.

Finally, the compatibility of these two techniques was tested by comparing their experimental results, most deviations coming to within  $\pm 3 \%$  and always emerging as lower than FBV uncertainty limits, which is the equipment evidencing the highest

uncertainty values. Therefore, good agreement between both viscometers has been shown.

### **Funding Sources**

Consejería de Educación de la JCyL for project VA295U14

### **ACKNOWLEDGMENTS**

J.Z.C. acknowledges the Secretaría Nacional de Educación Superior, Ciencia, Tecnología e Innovación (SENESCYT), Ecuador, for his doctoral studies scholarship, M.S. acknowledges the Ministerio de Educación (Spanish Government) for his FPU scholarship for doctoral studies. Authors acknowledge the Consejería de Educación de la JCyL for project VA295U14. We thank Prof. Trusler from Imperial College for providing us with the sensor.

### **REFERENCES**

- (1) W.A. Wakeham, A. Nagashima, J.V. Sengers, Measurement of Transport Properties of Fluid, Blackwell Scientific Publications, Oxford, 1991.
- (2) ISO/TR 3666. *Viscosity of Water*. 1998.
- (3) J.F. Swindells, J.R. Coe, T.B. Godfrey, Absolute Viscosity of Water at 20°C, J. Res. NBS 48 (1952) 1– 31.
- (4) M.J. Assael, C.P. Oliveira, M. Papadaki, W.A. Wakeham, Vibrating-Wire Viscometers for Liquids at High Pressures, Int. J. Thermophys. 13 (1992) 593 –615.
- (5) A.A.H. Pádua, J.M.N.A. Fareleira, J.C.G. Calado, W.A. Wakeham, Validation of an Accurate Vibrating-Wire Densimeter: Density and Viscosity of Liquids over Wide Ranges of Temperature and Pressure, Int. J. Thermophys. 17 (1996) 781– 802.

- (6) T. Retsina, S.M. Richardson, W.A. Wakeham, The Theory of a Vibrating-Rod Viscometer, *Appl. Sci. Res.* 43 (1987) 325–346.
- (7) S.S. Chen, M.W. Wambsganss, J.A. Jendrzejczyk. Added Mass and Damping of a Vibrating Rod in Confined Viscous Fluids. *J. Appl. Mechanics* 43 (1976) 325–329.
- (8) F.J.P. Caetano, J.M.N.A. Fareleira, C.M.B.P. Oliveira, W.A. Wakeham, New Measurements of the Viscosity Vibrating Wire Technique. *J. Chem. Eng. Data* 50 (2005) 1875–1878.
- (9) F.J.P. Caetano, J.M.N.A. Fareleira, C.M.B.P. Oliveira, W.A. Wakeham, Validation of a Vibrating Wire Viscometer: Measurements in the Range of 0.5 to 135 mPa·s. *J. Chem. Eng. Data* 50 (2005) 201–205.
- (10) D.R. Caudwell, J.P.M. Trusler, V. Vesovic, W.A. Wakeham, The Viscosity and Density of n-Dodecane and n-Octadecane at Pressures up to 200 MPa and Temperatures up to 473 K. *Int. J. Thermophys.* 25 (2004) 1339–1352.
- (11) F. Peleties, J.P.M. Trusler, Viscosity of Liquid Di-Isodecyl Phthalate at Temperatures between (274 and 373) K and at Pressures up to 140 MPa. *J. Chem. Eng. Data* 56 (2011) 2236–2241.
- (12) D. Caudwell, Viscosity of Dense Fluid Mixture. PhD Thesis; University of London, London, 2004.
- (13) J. Zambrano, Desarrollo de un Viscosímetro de Hilo Vibrante para la Caracterización Termofísica a Alta Presión de Nuevos Biocombustibles. PhD Thesis; University of Valladolid, Valladolid, 2014.

(14) Evaluation of Measurement Data - Guide to the Expression of Uncertainty in Measurement (JCGM 100: 2008); BIPM, 2008.

(15) P. Daugé, A. Baylaucq, L. Marlin, C. Boned, Development of an Isobaric Transfer Viscometer Operating up to 140 MPa. Application to a methane + decane system. *J. Chem. Eng. Data* 46 (2001) 823–830.

(16) M. Zeng, C. Schaschke, High Pressure Falling Sinker Liquid Viscosity Determination without Supplementary Density Data: A New Approach. *Int. J. Chem. Eng.* 2009 (2009) 1–8.

(17) M.J.P. Comuñas, X. Paredes, F.M. Gaciño, J. Fernández, J.P. Bazile, C. Boned, J.L. Daridon, G. Galliero, J. Pauly, K.R. Harris, Viscosity Measurements for Squalane at High Pressures up to 350 MPa from  $T = (293.15 \text{ to } 363.15) \text{ K}$ . *J. Chem. Thermodyn.* 69 (2013) 201–208.

(18) M.C.S. Chen, J.A. Lescarboua, G.W. Swift, The Effect of Eccentricity on the Terminal Velocity of the Cylinder in a Falling Cylinder Viscometer. *AIChE J.* 14 (1968) 123–127.

(19) C.J. Schaschke, S. Allio, E. Holmberg, Viscosity Measurement Of Vegetable Oil At High Pressure. *Food Bioprod. Process.* 84 (2006) 173–178.

(20) M. Sobrino, J.J. Segovia, Development of a Falling Body Viscometer Technique for Biofuels Characterization at High Pressure. *Dyna* 87 (2012) 438–445.

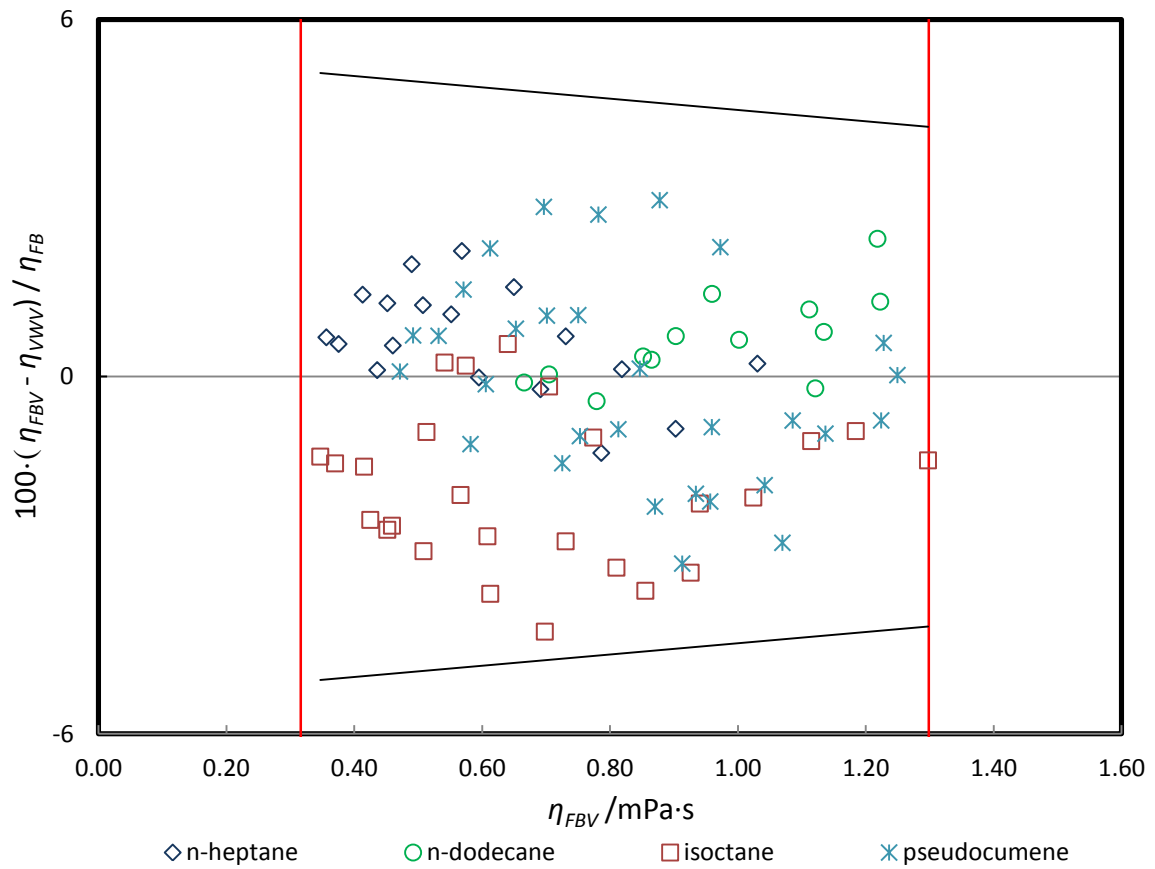
(21) M.J. Assael, H.M.T. Avelino, N.K. Dalaouti, J.M.N.A. Fareleira, K.R. Harris, Reference Correlation for the Viscosity of Liquid Toluene from 213 to 373 K at Pressures to 250 MPa. *Int. J. Thermophys.* 22 (2001) 789–799.

- (22) M.J. Assael, J.H. Dymond, M. Papadaki, P.M. Patterson, Correlation and Prediction of Dense Fluid Transport Coefficients. 1. *n*-Alkanes. *Int. J. Thermophys.* 13 (1992) 269–281.
- (23) F.M. Gaciño, M.J.P. Comuñas, T. Regueira, J.J. Segovia, J. Fernández, On the viscosity of two 1-butyl-1-methylpyrrolidinium ionic liquids: Effect of the temperature and pressure. *J. Chem. Thermodyn.* 87 (2015) 43–51.
- (24) I. Cibulka, L. Hnědkovský, Liquid Densities at Elevated Pressures of *n*-Alkanes from C5 to C16: A Critical Evaluation of Experimental Data. *J. Chem. Eng. Data* 41 (1996) 657–668.
- (25) A.S. Pensado, M.J.P. Comuñas, L. Lugo, J. Fernández, Experimental Dynamic Viscosities of 2,3-Dimethylpentane up to 60MPa and from (303.15 to 353.15) K Using a Rolling-Ball Viscometer, *J. Chem. Eng. Data* 50 (2005) 849-855.
- (26) C.K. Zéberg-Mikkelsen, G. Watson, A. Baylaucq, G. Galliero, C. Boned, Comparative experimental and modeling studies of the viscosity behavior of ethanol +C7 hydrocarbon mixtures versus pressure and temperature, *Fluid Phase Equilib.* 245 (2006) 6-19.
- (27) D.I. Sagdeev, M.G.Fomina, G.Kh. Mukhamdezyanov, I.M. Addulagatov, Experimental Study of the Density and Viscosity of *n*-Heptane at Temperatures from 298 K to 470 K and Pressure up to 245 MPa. *Int. J. Thermophys.* 34 (2013) 1-33.
- (28) J.H. Dymond, N.F. Glen, J.D. Isdale, Transport Properties of Nonelectrolyte Liquid Mixtures VII. Viscosity Coefficients for Isooctane and for Equimolar Mixtures of Isooctane + *n*-Octane and Isooctane + *n*-Dodecane from 25 to 100°C at Pressures up to 500 MPa or to the Freezing Pressure, *Int. J. Thermophys.* 6 (1985) 233-250.

(29) U.G. Krahn, G. Luft, Viscosity of Several Liquid Hydrocarbons in the Temperature Range 298-453 K at Pressures up to 200 MPa, J. Chem. Eng. Data 39 (1994) 670-672.

(30) A.A.H. Pádua, J.M.N.A. Fareleira, J.C.G. Calado, W.A. Wakeham, Density and Viscosity Measurements of 2,2,4-Trimethylpentane (Isooctane) from 198 K to 348 K and up to 100 MPa, J. Chem. Eng. Data 41 (1996) 1488-1494.

### Table of Contents Graphic



Comparison between the viscometers developed in the laboratory: Vibrating-Wire Viscometer and Falling-Body Viscometer.